Hindawi
Advances in Civil Engineering
Volume 2021, Article ID 1315849, 12 pages
https://doi.org/10.1155/2021/1315849

Research Article

Experimental Study on the Bending Behavior of Steel-Wood Composite Beams

Shaowei Duan, Wenzhao Zhou, Xinglong Liu, Jian Yuan, and Zhifeng Wang

College of Civil Engineering, Central South University of Forestry and Technology, Changsha, Hunan 410004, China

Correspondence should be addressed to Wenzhao Zhou; 931598651@qq.com

Received 7 January 2020; Revised 11 May 2021; Accepted 3 June 2021; Published 28 June 2021

Academic Editor: Cristiano Loss

This paper proposes a steel-wood composite beam with H-shaped steel beam webs glued to the wood. As a new type of composite beam, it combines the advantages of low energy consumption of wood, high permeability, and less pollution and the advantages of light weight and high strength of steel, high degree of assembly, short construction period, and less construction waste generated. Carrying out research is of great significance to improve the mechanical properties of steel-wood composite beams and promote the development of steel-wood composite structures. In this paper, three hot-rolled H-beam-larch composite beams and one pure steel beam were tested for bending capacity. The composite beams are divided into two different combinations of A and B types. The two sides of the web are connected with larch wood by structural glue to form a composite beam. The type B composite beam is a larch wood glued on both sides of the H-shaped steel web and penetrates the bolts at the same time. Through the three-point monotonic static grading loading of the composite beam, the deflection change, failure phenomenon, and form of the specimen during the experiment were observed. Under the circumstances, the ultimate bearing capacity of the test piece was changed to study the combined effect of larch and hot-rolled H-shaped steel. The results show that the overall performance of the H-shaped steel-larch composite beam is good. Bonding wooden boards on both sides of the steel beam web can improve the bearing capacity, and the form of the member is more reasonable and effective; increasing the cross-sectional size of the H-beam in the steel-wood composite beam can further improve the bearing capacity of the composite beam; adding bolt anchorage on the basis of the structural glue used in the composite beam can further improve the bearing capacity of the composite beam. The superposition principle is used to simplify the calculation of the ultimate bearing capacity of H-shaped steel-larch composite beams. Comparing the calculation results with the test results, the data are in good agreement, which can provide a design reference for the practical application of such composite beams.

1. Introduction

As a new structure, the steel-wood composite component can fully utilize the advantages of the two materials [1]. In this project, composite beams made of larch wood glued to both sides of hot-rolled H-shaped steel webs were selected as the object to study their bending mechanical properties [2–8]. H-shaped steel was used as the main force-bearing part, and H-shaped steel was glued to the two sides of the web. Providing sufficient lateral stiffness can improve the stability of the structure and at the same time improve the bearing capacity of the structure. Compared with the previous steel-wood composite beams, the H-shaped steel cladding is outside of the wood in this test, and the maximum stress point on the beam cross section appears on the H-shaped steel, which can give full play to the strength advantages of the steel. The purpose of carrying out the experimental research is to promote new structural members suitable for sustainable development, improve the mechanical performance of steel-wood composite beams, promote the development of steel-wood composite structures, and provide reliable data for future engineering practice [9–13].

In the research of steel-wood composite beams, Borri and Corradi [14, 15] carried out the flexural bearing capacity test of reinforced wooden beams with high-strength steel cable nets and calculated the flexural bearing capacity. Tests have shown that high-strength steel cable nets can improve the bending capacity of wooden beams. Vecchi et al. [16] studied prestressed glulam wood reinforced with steel bars. Compared with the unreinforced beams, the results show that the mechanical strength, bearing capacity, and stiffness

of the beams are enhanced. Jasien ko and Nowak [17] studied the bearing capacity of steel-wood composite beams. The results show that placing the steel plate on the inside or outside of the wooden beam improves the strength of the wooden beam. In addition, sandblasting on the joint surface of the steel plate and the wooden beam can also improve the joint strength of the component. Sandblasting on the bonding surface also improves the bonding strength of the component. Soriano et al. [18] studied the bearing capacity of reinforced steel-wood composite beams by bending bearing capacity test. The results show that the symmetric loading of steel bars onto laminated wooden beams can significantly improve the ultimate bearing capacity and stiffness of laminated wooden beams. Chen [19] conducted a study on the mechanical properties of the connection interface of the composite beam. An experimental study was conducted on the composite beam by changing the material of the screw, the diameter of the screw, and the distance between the screws. The research results show that the composite beam undergoes brittle failure in the case of simple screw connection and simple viscose connection interface, and the load bearing capacity of the interface is effectively improved in the case of screw and viscose mixed connection. Ghazijahani et al. [20] and others conducted experiments on light wood I-beams reinforced with composite materials. Through experiments and numerical methods, the bending and shear strength of lightweight composite wood I-beams are studied in order to use composite materials to strengthen I-beams and improve structural performance. The structural performance is improved by using composite materials to strengthen the I-beam. The experiment verified the efficiency of the developed reinforcement method, in which the carrying capacity was increased by 70%. In addition, compared to ordinary specimens, reinforced composite beams obtain a large amount of energy absorption and ductility.

In this paper, the hot-rolled H-beam is used as the skeleton. On the left and right outer surfaces of the hot-rolled H-shaped steel web, an epoxy resin structural adhesive or a bolt is used to consolidate the wooden board to form a composite beam of an H-shaped cross section as a research object. Its cross section is shown in Figure 1. The A-type is a section of the modern wood composite beam of the H-shaped steel web. The B-type section is made of H-shaped steel web and glued to the modern wood and simultaneously punched in the web. The bolts are tightened to form a composite beam section. The bending capacity test of steel-wood composite beams is carried out to study the combined effect of hot-rolled H-beam and modern wood. According to the test results, a simplified calculation formula of the bearing capacity of the steel-wood composite beam is proposed, which provided a theoretical basis for the practical application of the steel-wood composite beam.

2. Experimental Survey

2.1. Design and Production of Test Specimens. A total of four beams were produced in this test, and the test specimen L1 was a pure steel beam. L2–L4 are three H-shaped steel-wood composite beams, in which L2 and L3 are type A sections, and L4 is the type B section, as shown in Figure 2. The length of the four beam specimens is 3m, and the calculation span is 2.8 m. The specific test parameters are shown in Table 1. This test mainly studies the influence of the cross section dimensions of the composite beam, the presence or absence of internal rubber on the steel beam, and the presence or absence of welding bolts on the composite beam.

Larch glulam was used for wood, and its materiality test was completed in the laboratory of Central South University of Forestry and Technology. The strength is reduced according to wood defects (wood knots, cracks, etc.), and the reduction factor is taken as 0.6 [21]. The results are shown in Table 2. H-shaped steel is processed from Q235 steel, and its material property test is in accordance with the relevant requirements of "Metal material room temperature tensile test method." The sampling position and size design of the test specimen are provided by the manufacturer, and the test results are shown in Table 3.

2.2. Loading Device and Measuring Point Arrangement. The bending capacity test of the steel-wood composite beam of this test is carried out by simply supported beam loading, as shown in Figure 3. The average length along the beam length is divided into three sections using a two-point loading method. Theoretically speaking, the two ends are shear-bending sections, and the middle section is a purely curved section. In order to compare the mechanical properties of the combined beam flexural bearing capacity, among the four components designed in this test, L1 is a pure steel beam test piece, mainly as a comparative experimental beam, and its failure mode is mainly unstable failure; L2–L4 are steel-wood composite beam specimens with bending failure.

The test uses a 100 T reaction frame and a 100 T hydraulic jack. The load is measured by the load sensor. The weight of the distribution beam and the load sensor and the weight of the composite beam are not included in the test. The test beam is simply supported on the hinge support, and a steel sheet is placed between the test beam and the support to ensure uniform contact between the two contact surfaces and prevent local damage to the support. Two equivalent concentrated loads are applied at 900 mm from the support at both ends of the composite beam. The pure bend is 1000 mm long. Using the monotonic static grading loading method, each stage of the elastic stage is 1/10 of the estimated limit, the elastoplastic stage is 1/20 of the estimated limit, and the slow speed is added close to the ultimate load. Before each test, preload the test pieces to check whether the instruments are normal and the readings are stable. Wait for a while after each load is applied, record the strain and displacement, and record the crack development. One dial gauge is arranged in each of the span beam specimens, the concentrated force action point, the support, and the concentrated force action point 1/2. The arrangement of the measuring points is shown in Figure 4. Three strain gauges are arranged along the beam height on the web of the web

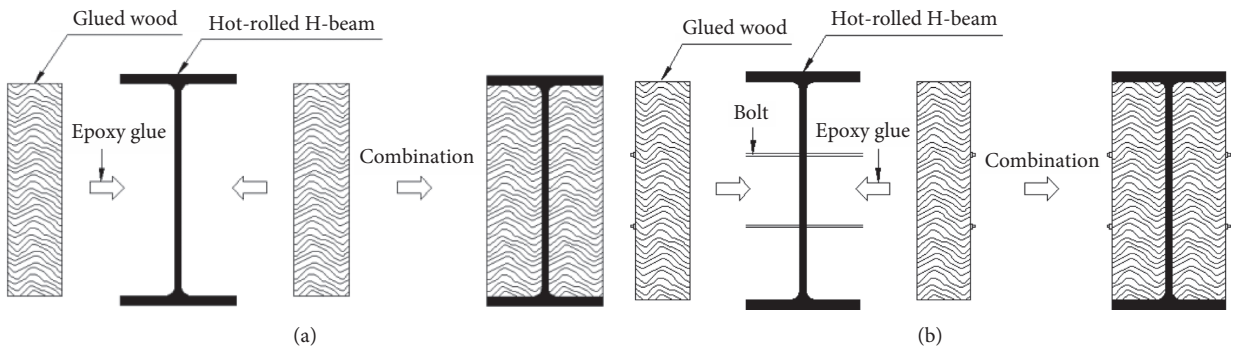

Figure 1: Composite beam section form. (a) Class A composite beam section. (b) Class B composite beam section.

Figure 2: Test beam.

Table 1: Main parameters of specimens.

Test piece number	Section form	t_f(mm)	t_w(mm)	h_w(mm)	t (mm)	b (mm)	l (mm)
L1	/	8	5.5	200	/	100	3000
L2	A	8	5.5	200	47.25	100	3000
L3	A	7	5	150	35	75	3000
L4	B	8	5.5	200	47.25	100	3000

Note. t_f, t_w, and $h_w$are the H-shaped steel flange thickness, web thickness, and height; t is the thickness of the board; b is the beam width.

Table 2: Material properties of wood.

Index	Airdry density (g·cm^{-3})	Modulus of elasticity parallel (MPa)	Bending strength parallel to grain (MPa)	Compression strength (MPa)
Experimental data	0.592	18571	72	43
Conversion value	—	—	43	26

Table 3: Elastic modulus of hot-rolled H steel.

Test number	Thickness (mm)	Yield strength (MPa)	Average yield strength (MPa)	Ultimate strength (MPa)	Average ultimate strength (MPa)	Elastic modulus (GPa)
1	6	262.95	260.41	376.19	399.88	203
2	6	263.87		378.15		
3	6	255.55		374.67		
4	7	259.51		423.95		
5	7	258.39		419.25		
6	7	262.18		427.04		

Figure 3: Loading device.

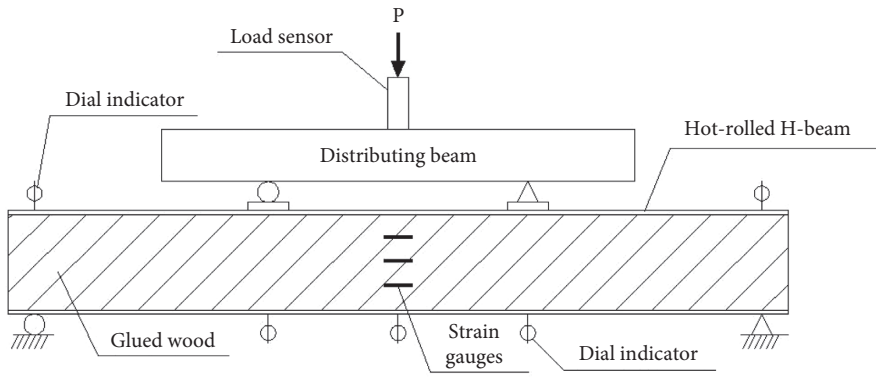

Figure 4: Layout of measuring points.

and the surface of the plank in the composite beam span. At the same time, a plurality of strain gauges is symmetrically arranged on the inner surface of the upper and lower flanges of the intermediate H-shaped steel and the outer surface of the upper and lower sides of the wood. A temperature-compensated strain gauge for steel and wood is placed at the instrument, and the strain gauge readings are collected using a Donghua 3818 static strain gauge, as shown in Figure 5.

3. Failure Process and Characteristics of Test Piece

3.1. Test Piece L1. The test piece L1 is a pure steel beam. After the test was started, the load reading decreased after loading to 100 kN, and the load could not be increased after 116 kN. At this time, the pure steel beam could not continue to bear. At the same time, the steel beam was bent downward, and the lateral bending would suddenly occur, resulting in instability and damage. The failure mode is shown in Figure 6.

3.2. Test Pieces L2 and L3. During the loading process of specimens L2 and L3, when in the elastic phase, the deflection of the composite beams increased linearly with the load; as the load gradually increased, the rubber layer peeling sound began to be heard, but the test piece did not show obvious damage, and then there was slight cracking in the middle of the beams; when the load reached the ultimate load, the fracture of the lower flange was observed, and the tensile crack occurred in the tension zone of the web. At this time, the beams could no longer carry, the loads were gradually reduced, the deformation continued to increase, and the specimen was bent and damaged at a midspan position. When the test pieces were unloaded, the test pieces produced a significant rebound deformation after unloading. The difference between L2 and L3 is that L2 has a continuous cracking sound when L2 reaches the limit load, while the L3 wood cracking sound is shorter and smaller. The test phenomenon is shown in Figures 7and 8.

3.3. Test Piece L4. During the loading process of the test piece L4, when in the elastic stage, the deflection of the composite beam increases linearly with the increase of the load. When the load reached 183.3 kN, the right side of the distribution beam began to degum, but the test piece did not show obvious damage. When the load reached 190.6 kN, the humming sound appeared. It was observed that the upper and lower flanges of the composite beam were degummed and cracked, and oblique cracks appeared at the edge of the bolt hole. When the load reached 205 kN, the load became smaller step by step, the deformation continued to increase, the deflection of the test piece was large, the steel plate under the distribution beam was deformed, and the specimen was

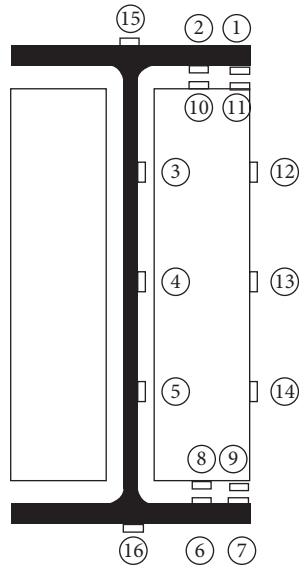

Figure 5: Midspan strain gauge layout.

(a) (b)

Figure 6: Failure mode of L1 test piece. (a) Lateral bending. (b) Instability failure.

(a) (b) (c)

Figure 7: Failure mode of L2 specimen. (a) Slight cracking in the middle. (b) Cracks in the web in tension area. (c) Bending failure.

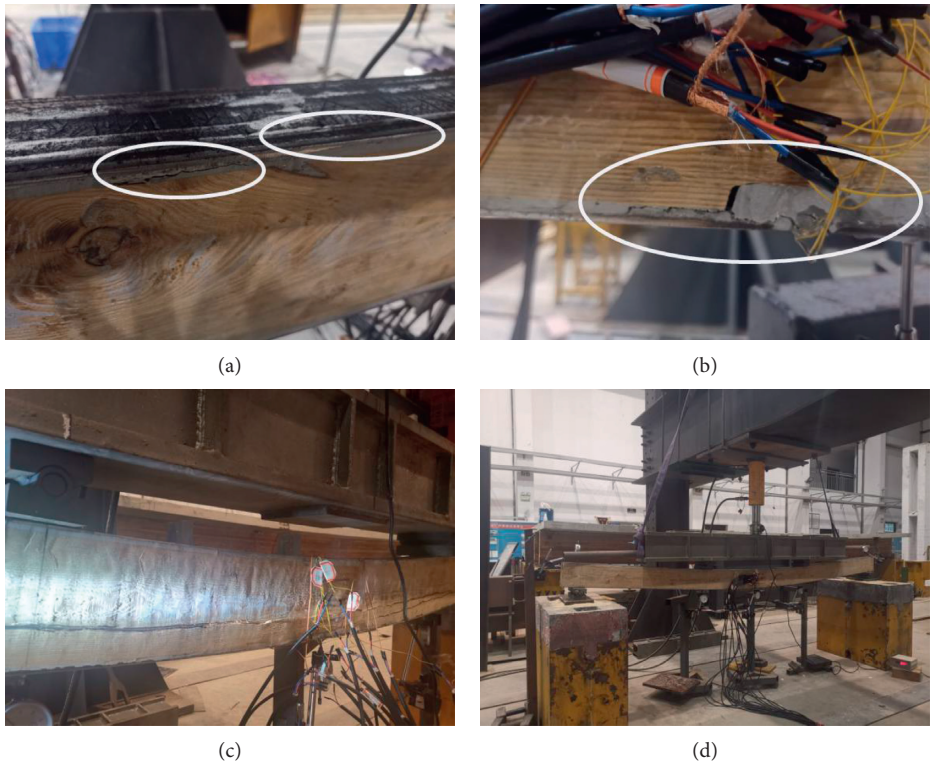

(a) (b) (c) (d)

Figure 8: Failure mode of L3 specimen. (a) Beginning of degumming. (b) Slight cracking in the middle. (c) Tension cracks in tension area. (d) Bending failure.

bent and broken at the midspan position. The test phenomenon is shown in Figure 9.

4. Analysis of Experimental Results

4.1. Load-Span Deflection Curve. According to the data collected by the data acquisition instrument, the load-span deflection curves of L1~L4 are plotted, as shown in Figure 10. It can be seen from Figure 10that the bending bearing capacity of L4 is the largest because L4 adds bolts to the glue in the web. Secondly, the bearing capacities of L2, L1, L3, and B composite beams are significantly higher than those of Class A composite beams. The load of L2 is larger than that of L1 because the web is glued to the web on the basis of the pure steel beam; the cross-sectional size of L1 is larger than L3, so the load is large. Before the buckling of the steel, the composite beam is in the elastic phase, and the load-span deflection curve increases linearly. When the deflection increases to a certain value, the beam will suddenly bend laterally and the lateral bending will suddenly cause the overall instability of the steel beam. The curve of specimen L2~L4 increases linearly at the initial loading stage. When the load increases to a certain extent, the slope of the curve gradually decreases, and the deformation speed of the composite beam increases. At this time, the web is observed. The wood board in the tension zone under the slab breaks, and tension cracks appear. The composite beam enters the elastoplastic stage. The stiffness of the composite beam gradually decreases until the composite beam loses its bearing capacity. The H-shaped steel-wood composite beam combined in this way has good performance. The ductility and deformation ability will not lose stability immediately after reaching the ultimate load and can give full play to the respective strengths of steel and wood.

4.2. Bending Moment Curvature Diagram. According to the test data, the function relationship between the deflection y of the composite beam and the length x is fitted, and then the curvature of the midspan of the beam under each load is calculated according to the formula, and finally the bending moment curvature diagrams of L1~L4 are made, as shown in Figure 11.

$$\varphi = \frac{1}{\rho}, \quad = \frac{d^2 y}{dx^2}, \tag{1}$$

where $\varphi$is the curvature of the midsection of the composite beam; $\rho$is the radius of curvature of the composite beam at that point; $x$is the length of the composite beam; and $y$is the deflection of the composite beam.

4.3. Test Beam Overall Deformation Curve. According to the data collected by the data acquisition instrument, the overall deformation curve of the test pieces L1~L4 is drawn, as shown in Figure 12.

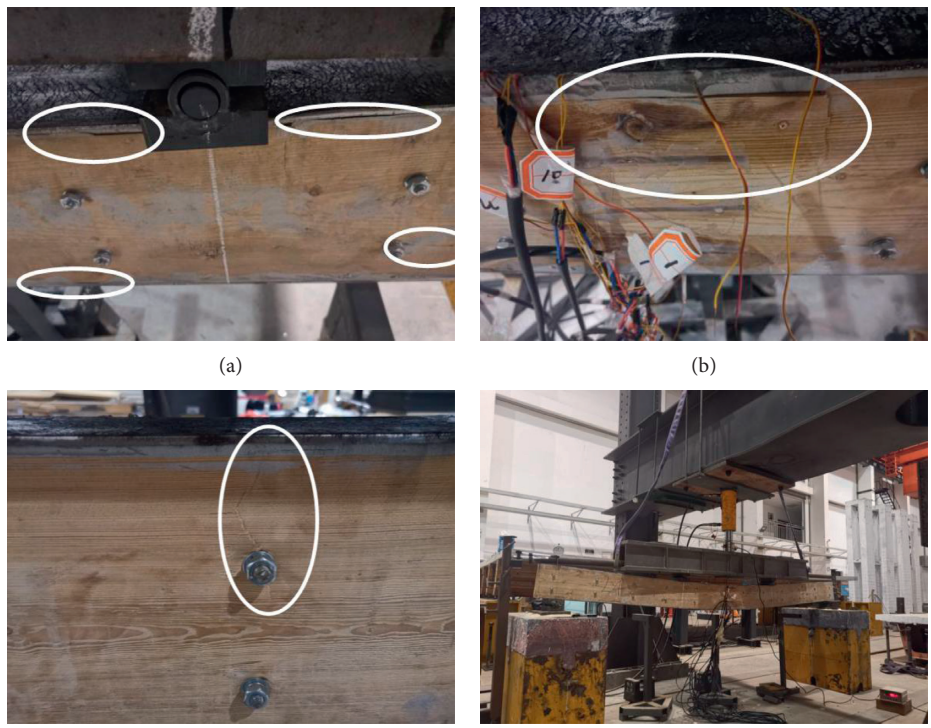

(a) (b) (c) (d)

Figure 9: Failure mode of L4 test piece. (a) The right support begins degumming. (b) The upper flange is degummed and cracked. (c) Oblique crack at the edge of the bolt hole. (d) Bending damage.

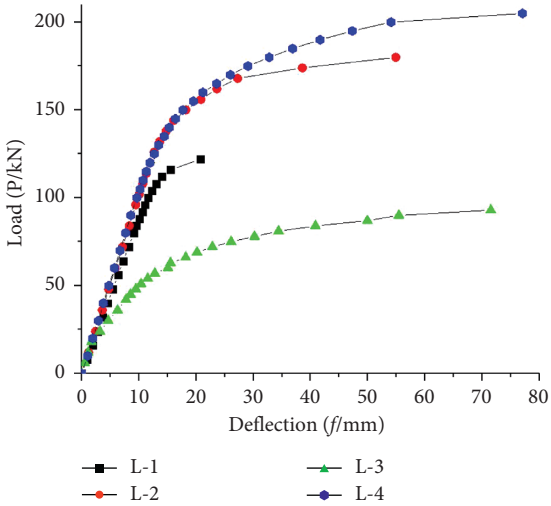

Figure 10: Load deflection curve.

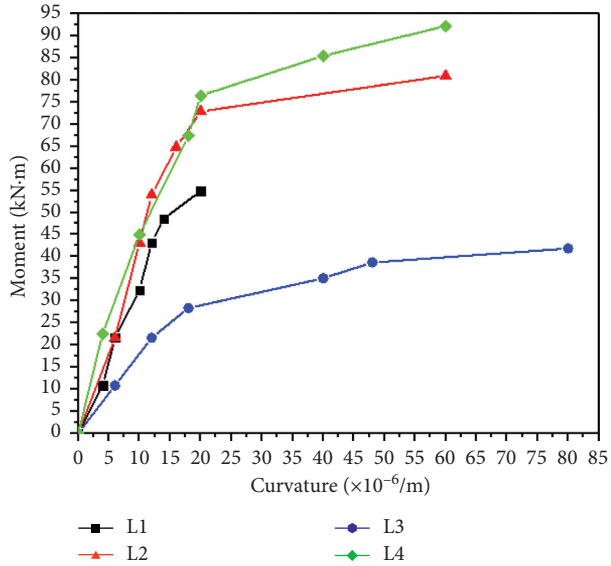

Figure 11: Bending moment curvature diagram of midspan.

It can be seen from Figure 12that the L4 specimen has the largest deflection, followed by L3 and L2, and the L1 specimen has the smallest deflection. Throughout the loading and failure process, the deformation of the specimen is basically symmetrical. In the initial stage of loading, the test beam is in the elastic stage. The deflection of the beam increases linearly with the increase of the load. The two ends of the test beam support will bend upward due to the three-point loading. The integrity of the composite beam is good; as the load continues to increase, the test beam enters the elastoplastic stage, the steel plate and the wood board begin to degum and peel off, the wood board begins to display transverse cracks, the steel plate buckles, and diagonal cracks appear around the bolts, causing the bolts to gradually lose its effect, the deflection of the test beam will increase at an accelerated rate in the later stage of loading, until the specimen is damaged, and the wood

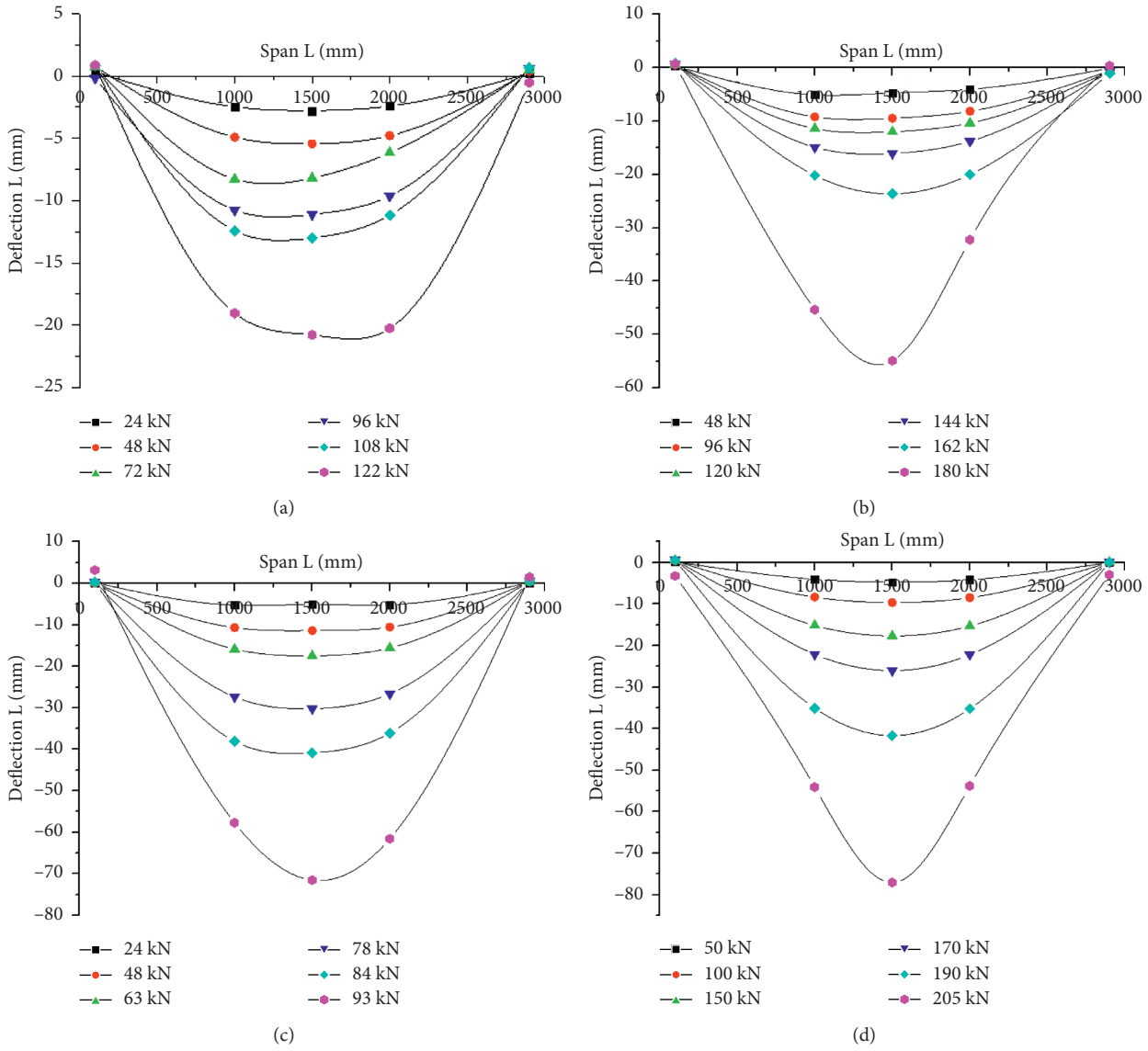

Figure 12: Test beam overall deformation curve. (a) L-1, (b) L-2, (c) L-3, (d) L-4.

and H-section steel have given full play to their respective advantages during the entire test.

4.4. Trans-Middle Section Load-Strain Relationship Curve. The load-strain relationship curves of the H-beam-wood composite beam No. 3, No. 5, No. 15, and No. 16 are shown in Figure 13. From left to right, this is the load-strain curve of L1, L2, L3, and L4. In the figure, the left half of the coordinate axis is the compression zone, the strain value is negative, the right half is the tension zone, and the strain value is positive. It can be seen from the curve in the figure that with the increase of the load, the strain values of each measurement increase linearly, and the curve appears to be outwardly offset. The curves of the compression zone and the tension zone are symmetrically distributed.

From the load-strain curve of the four beams in Figure 11, it can be seen that the load-strain curve of the specimen has a linear relationship at the initial stage of loading. At this stage, the composite beam is in the elastic working stage and the overall working performance is good. As the load continues to increase, the strain has a significant increase in the case of a small load amplitude, and the load-strain relationship exhibits a typical nonlinear law. When the load is close to the ultimate load, the opening condition of the cemented surface is expanding, and the tensile crack occurs in the tension zone of the web. The test piece loses the bearing capacity and the test is over.

The strain of the steel plate develops synchronously during the whole loading process of the B-type cross section test piece. The height of the upper and lower flanges of the section steel is always greater than the internal strain. This shows that the combination of structural glue and bolts is good for larch boards and hot-rolled H-beams. The composite beam has excellent overall performance when subjected to loads. The load-strain curve changes substantially

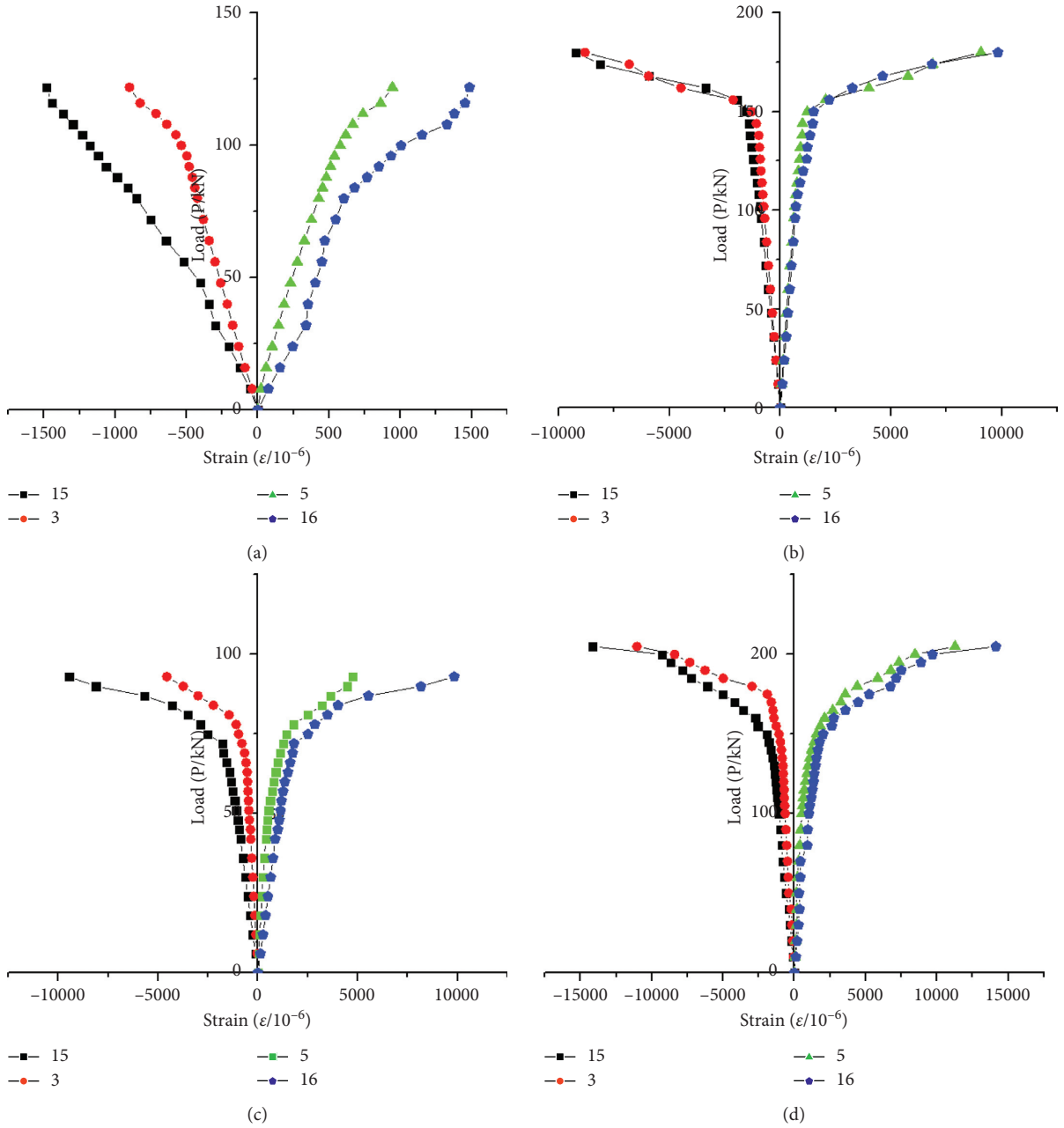

Figure 13: Load-strain relationship curve of midspan section. (a) L-1, (b) L-2, (c) L-3, (d) L-4.

linearly at the beginning of loading; as the load continues to increase, the strain increases significantly with a small load amplitude. When the load is close to the ultimate load, oblique cracks appear at the edge of the bolt hole, the bolt loses its effect, and the transverse crack occurs in the tension zone of the web, and the test piece loses its bearing capacity.

5. Theoretical Analysis of Bending Performance of H-Shaped Steel-Wood Composite Beam

In the theoretical analysis of this section, the following assumptions are made:

(1) The curvature of the H-shaped steel is the same as that of larch. The strain of the cross section will change along the height according to its linear distribution. After the composite beam is bent, its cross section will remain flat.

(2) Regardless of the combined effect between H-shaped steel and glulam, the bending stiffness and flexural bearing capacity of the section are calculated using the simple superposition principle.

5.1. Section Bending Rigidity Calculation. The section bending stiffness refers to the ability of the material, which resisted bending deformation by the product of the modulus

of elasticity of the material and the moment of inertia of the section of the curved member about its axis. The bending stiffness of H-beam-wood composite beams is calculated according to formula (2), and the bending stiffness of each beam in Table 4 is obtained. The obtained value can be brought into formula (3) to continue the calculation.

$$EI = E_w I_w + E_s I_s, \tag{2}$$

where E is the elastic modulus of the composite beam; I is the moment of inertia of the combined beam on the mandrel; E_w and E_s are the elastic moduli of the wood and H-shaped steel, respectively, which are taken to the measured values of the material test; and I_w and I_s are the moments of inertia of wood and H-shaped steel, respectively.

5.2. Calculation of the Load Value Corresponding to the Normal Service Limit State. Substituting formula (2) into the calculation formula of the simply supported beam deflection, the calculation formula of the midspan deflection of the steel-wood composite beam under normal use condition is

$$\delta = \beta S \frac{PaL2}{48EI}\left(3 - 4\alpha^2\right), \tag{3}$$

where δ is the allowable value of the deflection of the composite beam, $\alpha = a/L$, α is the distance from the concentrated force point to the proximal support, L is the combined beam span, and β_S is the deformation development coefficient of the steel-wood composite beam. When $L \le 3$, β_S takes 1.2.

In the normal service limit state, in order to ensure the function of the component, the mid-span deflection of L1~L4 should be within the control value. According to the steel structure design specification and the wood structure design specification, the deformation control condition of the composite beam in the normal use phase is $L/250$. The span of the test composite beam is 2800 mm, that is, the allowable deflection of the composite beam is 11.2 mm. According to formula (3), the load P_f when the composite beam reaches the allowable deflection value can be calculated correspondingly. When L1~L4 reach the allowable deflection of 11.2 mm in the test, the corresponding midspan load value P_e can be found from the load-span deflection curve in Figure 10.

It can be seen from Table 5 that the error between the theoretical value and the test value of the load corresponding to the test piece L-2~L-4 in the normal service limit state is within 10%, and the error between the theoretical value and the test value is relatively small.

5.3. Bending Capacity. During the test, the H-shaped steel beam L-1 showed instability and failure, so the flexural bearing capacity of the H-shaped steel beam L-1 needs to be calculated according to the overall stability of the flexural member; according to the "Steel Structure Design Code" (GB50017-2017) [22], the calculation formula of its bending capacity is as follows:

$$M_x \le \phi_b \gamma_x f W_x, \tag{4}$$

where M_x is the maximum bending moment acting around a strong axis; W_x is the modulus of beam cross section determined by compression fibers; and ϕ_b is the overall stability factor of the beam.

The overall stability coefficient of the beam should be as follows:

$$\phi_b = \frac{1}{\left(1 - \lambda_{b0}^{2n} + \lambda_b^{2n}\right)^{(1/n)}} \le 1.0,$$
$$\lambda_b = \sqrt{\frac{\gamma_x W_x f_y}{M_{cr}}}, \tag{5}$$

where M_{cr} is the critical moment of elastic buckling of simply supported beams, cantilever beams, or continuous beams; λ_{b0} is the initial general slenderness ratio with stability factor less than 1.0 (take 0.4); n is the index, $n = 2.5\sqrt[3]{b_1/h}$; b_1 is the width of I-shaped section compression flange; and h is the distance between the upper and lower flanges.

The bearing capacity superposition method is to calculate the respective bending bearing capacity of the two parts of the composite beam, H-shaped steel, and wooden board and then superimpose. The calculation formula of the bending section bearing capacity of the steel-wood composite beam is as follows:

$$M = M_w + M_s,$$
$$M_w = \sigma_w W_w, \tag{6}$$
$$M_s = \gamma W_n f_y,$$

where $M$is the bending capacity of the composite beam; $M_w$and $M_s$are the bending capacities of the wood and H-shaped steel in the composite beam, respectively; W_w is the section resistance moment of the wood in the composite beam; W_n is the net section modulus of the H-shaped steel in the composite beam; σ_w is the flexural strength of wood, which is taken according to the measured value of the material property test; f_y is the yield strength of H-shaped steel, which is taken according to the measured value of the material property test; and $\gamma$is the plastic development coefficient of steel, taking $\gamma = 1.05$ [23].

The test formula for the ultimate flexural capacity of H-beam-wood composite beams is as follows:

$$M_{\exp} = \frac{aP}{2}, \tag{7}$$

where a is the concentrated force action point at the proximal support distance and P is the concentrated load under the limit of the bearing capacity.

Table 5 shows the comparison between the calculation results of the bending capacity of test pieces L-1~L-4 and the test results. It can be seen from Table 5that the average error of the flexural bearing capacity of the four groups of test pieces is about 6.8%, and the average value of the contribution rate of the wood bearing capacity (Mw/Mcal) in the composite beam is about 50%. Lifting has a greater effect (Table 6).

Table 4: Bending stiffness of composite beam.

Test piece number	I_w (cm^4)	I_s (cm^4)	E_wI_w ($\times 10^8 N \cdot mm^2$)	E_sI_s ($\times 10^8 N \cdot mm^2$)	EI ($\times 10^8 N \cdot mm^2$)
L-1	/	1880	/	38164	38164
L-2	0.49	1880	6348.5	38164	44512.5
L-3	0.15	679	1898.9	13783.7	15682.6
L-4	0.49	1880	6348.5	38164	44512.5

Table 5: Comparison of the theoretical and experimental values of the load corresponding to the normal use limit state.

Test piece number	Theoretical value P_f(kN)	Test value P_e(kN)	P_f/P_e
L-1	112.4	96.7	1.16
L-2	131.1	121	1.08
L-3	46.2	50.1	0.92
L-4	131.1	120.4	1.08

Table 6: Comparison of bending bearing capacities between calculation and test results.

Test piece number	Mw (kN·m)	Ms (kN·m)	Mcal (kN·m)	Mexp (kN·m)	Mcal/Mexp	Mw/Mcal
L-1	/	48.4	48.4	47.25	1.02	/
L-2	46.4	48.3	94.7	81	1.16	0.4 9
L-3	22.4	20.4	42.8	41.85	1.02	0.52
L-4	46.4	48.3	94.7	92.25	1.03	0.49

Note. M_{cal} and M_{exp} are the calculated and experimental values of the bending moments of the specimen under the limit of bearing capacity.

6. Conclusion

In view of the fact that there are few studies on the bearing performance of H-shaped steel-wood composite beams and the H-shaped steel beams are prone to the problems of poor ductility and instability caused by local buckling, this paper studies this problem and designs H-shaped steel-wood composite beams with glued glulam for webs. In this paper, the bending performance of three H-steel-larch composite beams and one pure steel beam was tested. They have different combinations, different wood thicknesses, and different H-section cross-sectional dimensions. The failure process and failure morphology of the hot-rolled H-beam-larch composite beam were analyzed, and the relationship between deflection, strain, and load applied by the specimen was obtained. The theoretical analysis of the bending performance of the H-shaped steel-wood composite beam is made, and the calculation formulas of section bending stiffness, midspan deflection, and bending bearing capacity are proposed. Compared with the test results, the data are not much different, which verify the rationality of the theoretical calculation method. In summary, the main conclusions of this article are as follows.

This article mainly designs two types of composite beams of A and B. Among them, the type A combination is H-shaped steel web glued with modern wood to form the composite beam, and the type B combination is the H-shaped steel web glued on both sides. Larch wood is bonded with structural glue, holes are drilled at a certain distance on the web, and bolts are added to form a composite beam. Type A composite beams and type B composite beams have different forms of failure. For type A composite beams, the main cause of failure is that the load is loaded to a certain degree and the structure between the steel plate and the wood is unstuck and the structural failure occurs. The performance of the damaged steel plates and wooden boards has not reached the limit; for the type B composite beams, due to the anchoring effect of the bolts, there is basically no debonding between the H-shaped steel and the wooden boards, and they can work together from beginning to end. The cracks in the tension zone of the lower part of the midwebs are broken and the boards are rendered useless. The flexural bearing capacity of the composite beam is improved to avoid lateral instability and damage. The strength of wood and steel is fully utilized during the test, and the combination effect is significant.

According to the test results, adding wood planks on both sides of the pure steel beam web can improve the stability of the beam and thereby improve the bearing capacity; adding bolt anchoring to the steel-wood composite beam can well improve the glue-opening phenomenon between the steel and the section steel, thereby improving the bearing capacity of the composite beam; increasing the cross-sectional size of the H-shaped steel in the steel-wood composite beam can also improve the bearing capacity of the composite beam.

In this paper, the calculation formulas of section bending stiffness, midspan deflection, and bending bearing capacity are proposed. Among them, the principle of superposition is used to calculate the bending bearing capacity of composite beams. The force is then added to obtain the flexural bearing capacity of the composite beam. The result calculated by this method is not much different from the experimental value, which proves that this calculation method is reasonable.

Data Availability

The data used to support the findings of this study are available from the corresponding author upon request.

Conflicts of Interest

The authors declare that they have no conflicts of interest.

Acknowledgments

This study was supported by the Hunan Provincial Innovation and Entrepreneurship Technology Investment Project (no. 2019GK5087) and National Natural Science Foundation of China (nos. 51578554 and 51274258).

References

[1] F. Chao, *Research on Static Performance of Steel-Wood Composite Connection*, Beijing Jiaotong University, Beijing, China, 2015.

[2] Z. Li, *Flexural Performance Analysis of Steel-Bamboo Box Composite Beams*, Beijing Forestry University, Beijing, China, 2016.

[3] Y. Xu, *Research on Seismic Performance and Design Method of Steel-Frame Beam-Column Weak-Axis Joints with Concrete Floors*, Changan University, Xi'an, China, 2018.

[4] J. Li, *Research on Mechanical Properties of New Prestressed Steel-Wood Composite Columns*, Southwest University of Science and Technology, Mianyang, China, 2019.

[5] X. Wang, "Research status and development prospects of steel-wood composite structure," in *Proceedings of the 2011 National Annual Conference on Steel Structure*, Jacksonville, FL, USA, February 2011.

[6] Y. Xu, *Application Research of Steel Structure Residential Structure System*, Beijing Jiaotong University, Beijing, China, 2014.

[7] S. Du, *Technical Research of Steel Structure Residence*, Tsinghua University, Beijing, China, 2003.

[8] G. Liu, *Research on the Multi-Story Steel Structure Residential Structural System and Beam-Column Joints*, Central South University, Changsha, China, 2008.

[9] F. Ding, *Research on Mechanical Performance and Design Method of Concrete-Filled Circular Steel Tube Structure*, Central South University, Changsha, China, 2006.

[10] G. Meng, *Research on the Flexural Performance of Partially Prestressed Steel Reinforced Ultra-High-Strength Concrete Beams*, Dalian University of Technology, Dalian, China, 2006.

[11] C. He, *Research on the Flexural Performance of Outsourcing U-Shaped Steel-Concrete Composite Beams*, Harbin Institute of Technology, Harbin, China, 2014.

[12] Y. Ding, *Research on the Design and Construction Mode of High-Rise New-Type Industrialized Residence*, Southeast University, Dhaka, Bangladesh, 2018.

[13] J. Luo, *Research on the Commercialization of Architectural Composition Order from the Perspective of Architectural Industrialization*, Southeast University, Dhaka, Bangladesh, 2018.

[14] A. Chen, D. Li, C. Fang, Q. Zheng et al., "Experimental study on bending behavior of H-shaped steel-wood composite beams," *Journal of Building Structures*, vol. 37, no. S1, pp. 261–267, 2016.

[15] A. Borri and M. Corradi, "Strengthening of timber beams with high strength steel cords," *Composites Part B Engineering*, vol. 42, no. 6, 2011.

[16] A. D. Vecchi, S. Colajanni, R. Deletis, A. Catanese, and S. Iudicello, "Reinforced glulam: an innovative building technology," *International Journal for Housing Science*, vol. 32, no. 3, pp. 207–211, 2008.

[17] J. Jasien´ko and T. P. Nowak, "Solid timber beams strengthened with steel plates-experimental studies," *Construction and Building Materials*, vol. 63, pp. 81–88, 2014.

[18] J. Soriano, B. P. Pellis, and N. T. Mascia, "Mechanical performance of glued-laminated timber beams symmetrically reinforced with steel bars," *Composite Structures*, vol. 150, 2016.

[19] K. Chen, *Research on the Mechanical Properties of the Interface of Thin-Wall H-Shaped Steel-Wood Composite Beams*, Southwest University of Science and Technology, Mianyang, China, 2019.

[20] T. G. Ghazijahani, T. Russo, and H. R. Valipour, "Lightweight timber I-beams reinforced by composite materials," *Composite Structures*, vol. 223, 2020.

[21] W. Long and X. Yang, *Wood Structure Design Manual*, China Building Industry Press, Beijing, China, 2005.

[22] China Standard Press, *Design Standards for Steel Structures*, China Standard Press, Beijing, China, 2017.

[23] *Building Structure Static Calculation Manual*, China Building Industry Press, Beijing, China, 2000.